Efficient Design of Ultrasound True-Velocity Flow Mapping

Yasser M. Kadah and Ahmed H. Tewfik
Biomedical Engineering Program
University of Minnesota

Ultrasound imaging is one of the most prominent noninvasive imaging modalities currently in use. Its applications extend from plain soft-tissue imaging, as in abdominal sonography, to laparoscopy and blood flow/perfusion mapping. Blood-flow mapping is one of the most important applications of ultrasound. In this application, 2D maps of blood velocity values are generated and displayed atop B-mode ultrasound images to correlate with the underlying anatomy (Fig. 1). The velocity values are color-coded in red or blue to distinguish them from the usual gray-scale used for B-mode ultrasound images. The *red-scale* is used for velocity values directed toward the transducer while the *blue-scale* is used for those directed away from the transducer. These types of flow maps with this particular color coding are usually referred to as *color Doppler images*. These images are of great value in many diagnostic applications, such as echocardiography and perfusion imaging. Also, their potential in novel tumor-detection techniques, such as sonoelasticity, and for adding a new flow dimension to quantitative tissue characterization is currently under investigation [1-2].

In general, currently available techniques for generating flow maps can be classified into two main categories: *frequency-domain techniques* and *time-domain techniques*. Both classes have their relative advantages and disadvantages as they try to provide solutions to the common problems of flow mapping, such as limited velocity estimation accuracy and mapping resolution. Nevertheless, the conventional forms of both techniques share one major limitation in that they are able to map only one or two components of the 3D flow velocity in using 1D transducers. Given the random orientation of flow velocities at different locations throughout the image plane, it is obvious that the resulting flow maps consist of velocity values that cannot be directly compared since they do not have the same reference. This problem has profound effects on the diagnostic abilities of the techniques and certainly can prevent quantitative characterization of image regions. To be able to solve the problem of creating true-velocity maps, we have to go back and revise our classical velocity estimation models and propose more general models instead.

In this article, we describe the general theory of the classical Doppler technique for flow mapping and show that its main assumptions do not generally hold for ultrasound imaging. We then develop a generalized model for frequency-domain flow mapping in practical ultrasound imaging situations. Using this model, we show that it is possible to compute the true velocity from single-aperture configurations. We discuss improving the resolution and velocity estimation accuracies and propose a novel approach based on a generalization of the radar-ambiguity function model. We also consider the same problems for time-domain techniques. We propose a generalization of the correlation technique that takes into account the ultrasound field effect, and show that it is theoretically possible to obtain true-velocity flow maps from single-aperture configurations. Finally, we discuss the relative advantages and disadvantages of both frequency-domain and time-domain techniques.

Frequency-domain Flow Mapping

Let us consider the class of methods that derive flow maps directly from the power spectrum of the received pulse-echo-mode ultrasound signal. The traditional way of doing this is to use the Doppler equation, which has the form:

$$f_D = 2\frac{v \cdot \cos\phi \cdot f_T}{c}$$

Here, f_D is the frequency shift between the received signal and the transmitted signal, v is the true-flow velocity, c is the velocity of ultrasound in tissues, f_T is the transmitted

 0739-5175/96/$5.00©1996 September/October 1996

1. An example of a color Doppler image. The gray-scale is used for the B-mode intensity while the red and blue scales are used to represent flow velocities.

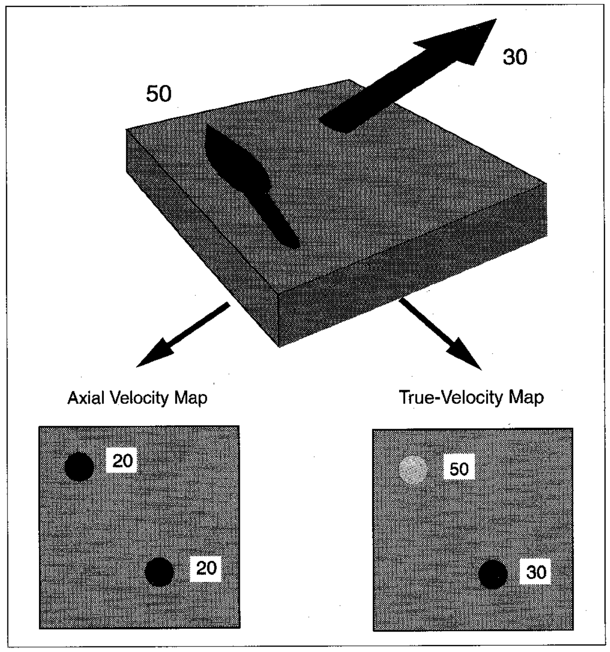

2. Illustration of the problem of axial velocity mapping. Different size vectors map to the same value and only true-velocity mapping can show the actual values.

frequency, and ϕ is the angle between the direction of flow and the transmitter/receiver transducer axis. Given the transmitted frequency and assuming the velocity of ultrasound in tissue to be constant and equal to 1540 m/s, the true-flow velocity value can be estimated from the Doppler equation by measuring the frequency shift and the exact 3D geometry of the problem, as characterized by ϕ. Unfortunately, the geometry of the problem is usually not available and quite difficult to assess. As a result, the above equation can be used to estimate the projected velocity vector, $v \cos \phi$, which represents the component of the true velocity in the direction of the transducer axis, or *axial velocity* (Fig. 2). It follows that computation of the true velocity using this method would theoretically require at least three non-coplanar transducers to be able to reconstruct the 3D magnitude from three independent projections.

The Doppler equation suffers from a number of major problems that can greatly limit its value for flow-mapping applications. It is derived under the assumption of monochromatic plane wave excitation. Hence, it may not be valid in describing practical ultrasound imaging situations. Although this condition can be approximately satisfied with a very small transducer and a very long excitation signal, the resultant system cannot be used in flow mapping because of its extremely poor resolution in both range and azimuth. As a result, the effects of finite transducer size and excitation length appear in the form of distortions in the computed power spectrum. These distortions are commonly known as *geometric* and *transit-time broadening* effects, respectively [2]. Another problem with the Doppler model is the complexity of the practical implementation of true-velocity estimation systems from multiple transducer configurations. Temporal and spatial registration, in addition to limited vessel accessibility, are examples of the problems encountered in this area. For these reasons, the currently available flow-mapping techniques based on the Doppler model provide an axial velocity map instead of the more convenient true-velocity map.

Generalized Power-spectrum Model

Consider now a more general model for the process of ultrasound flow mapping (Fig. 3). In this model, we do not assume particular forms for the ultrasound field and excitation signal. We only assume that Fresnel propagation conditions are satisfied [3]. We proceed to derive an analytical expression for the power spectrum of the received signal as a function of the imaging conditions, as modified by the 3D flow (Fig. 4). Given this expression, we can then consider the problem of estimating the true-velocity parameters by measuring the power spectrum. In deriving our model, we try to associate all assumptions with known physical quantities/phenomena in the actual process.

In laminar flow, blood, consisting of plasma and formed elements, moves in a particular direction with uniform velocity. Given that the plasma itself is a homogeneous fluid, we do not expect to receive any reflection/scattering phenomena from ultrasound waves propagating through this medium. On the other hand, the formed elements — mainly red blood cells (RBC) — will be a source of scattering. This scattering can generally be assumed to be uniform (Rayleigh) scattering [4]. It is usually of very weak intensity, and that is the reason why the inside of blood vessels appear dark in B-mode images. Nevertheless, this scattering phenomenon is the sole source of information for velocity estimation in flow mapping. In uniform flow, the RBCs will be distributed fairly uniformly in the volume inside the vessel, in a random but fixed fashion for any given small period of time. Even though the randomness assumption is not hard to justify, the assumption of a fixed pattern may need some explanation. A time-varying pattern inside a uniform flow must be due to space-varying local forces inside the moving fluid that can act on the solid blood elements to cause their relative motion and, hence, their change in the moving pattern. Forces of this nature are usually associated with flow acceleration, which is not the case in our situation. In other words, our model holds for brief time intervals during which the assumptions of constant velocity and zero acceleration are both valid. In this case, we may view

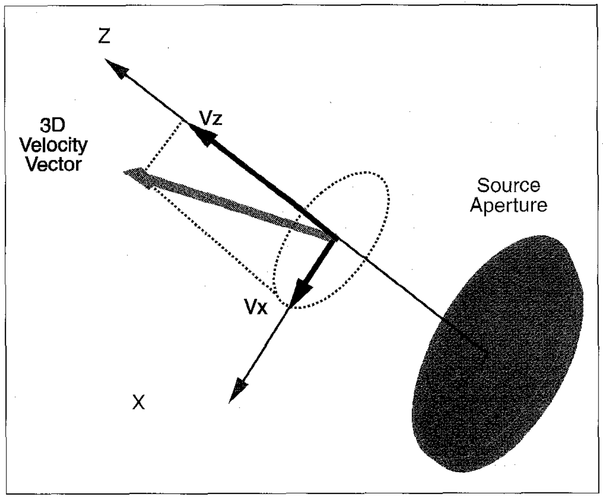

3. The geometry of the flow-mapping problem.

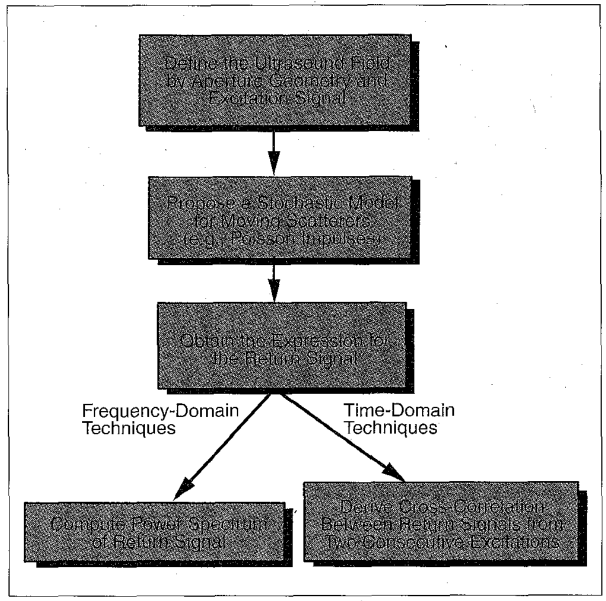

4. Block diagram of the generalized power-spectrum model derivation.

the pattern of RBCs as a large but finite collection of parallel straight lines of ideal Rayleigh scatterers. The distributions of the scatterers along these lines are assumed to be independent and identically distributed with a Poisson impulses random distribution. Under the conditions of Fresnel propagation, the return power spectrum from a a single line of moving scatterers takes the form [5]:

$$\Phi_{RR}(\omega) = \frac{\lambda' \sigma_s^2}{\left(v_x(1+2\frac{v_z}{c})\right)^2} \cdot \left| U\left(\frac{\omega}{v_x}\right) * S\left(\frac{\omega}{1+2\frac{v_z}{c}}\right) \right|^2$$

where $\Phi_{RR}(\omega)$ is the power spectrum of the received signal; λ' is a function of the Poisson model parameter; σ_s is the scattering cross-section of the effective scatterers; c is the phase velocity of ultrasound in tissues; v_x and v_z are the transverse and axial velocities, respectively; $U(\cdot)$ is the Fourier transform of the effective transmit/receive field along the line of motion; and $S(\cdot)$ is the Fourier transform of the excitation signal. From this expression, we can see that the axial velocity appears as a scaling of the excitation signal, while the lateral velocity appears as a scaling of the beam pattern. Scaling means dilation or shrinking of the original function. The effect of velocity values on the magnitude of the power spectrum is of little use without a reference magnitude for comparison.

The above description suggests that these scaling effects can be measured by observing the power spectrum and choosing the velocity parameters by directly fitting this observed spectrum to the model. This is not possible, in general, in practical situations, since the received echo is the superposition of the return from many lines of scatterers experiencing different fields. It is easy to see that space shift variations in the power spectrum shape are quite complex and mathematically intractable in practical situations where the spatial extension of the volume of moving scatterers is not known. As a result, we must find common features among all flow lines, which are only functions of the velocity parameters, given some general description of the field at the depth of the flow.

Two main approaches have been proposed to solve the problem of spatial variation. The first is to assume that the flow volume is small compared to the field at the depth of flow, and therefore the field at all lines is basically the same. This approach can be quite restricting in many cases. For example, if the flow is in the focal plane of a thin lens in the usual transducer-against-lens configuration, or is in the far field [6-7], the field has a quadratic phase term. This quadratic phase term requires the flow to be in the center of the field, in addition to being extremely localized away from the areas of the field where the phase variations cannot be overlooked. Moreover, the extension of the flow in the axial direction should be very limited to be able to assert range invariance. Therefore, we propose a more flexible approach to ensure range and lateral-flow-shift invariance [8]. In this approach, we design the field such that its angular spectrum is of compact support. This condition does not imply that the field will be the same for all lines anywhere in the image plane. However, it ensures that some basic properties of the measured power spectrum, such as its bandwidth and frequency shift, will be space-invariant. Given that these properties are measurable and can be directly related to the velocity parameters, the process of velocity estimation can be transformed into a space-shift-invariant problem (Fig. 5).

Another important observation can be made from the generalized model. If the excitation field is chosen to be circularly symmetric, it is clear to see that the x-axis of our model can be arbitrarily selected to be the direction of the projection of the true velocity onto the transverse plane. As a result, the estimated axial and lateral velocity components are basically the only two components of the true-velocity vector. Therefore, the true-velocity magnitude can be obtained once these two components are computed. Consequently, it becomes possible, in principle, to generate true-velocity maps from single coplanar aperture configurations.

Improvement of Frequency-domain-based Flow Mapping

As in all measurement procedures, the parameter estimates deviate from their true values. The estimation errors can be essentially divided into two major sources: *systematic* (*determi-*

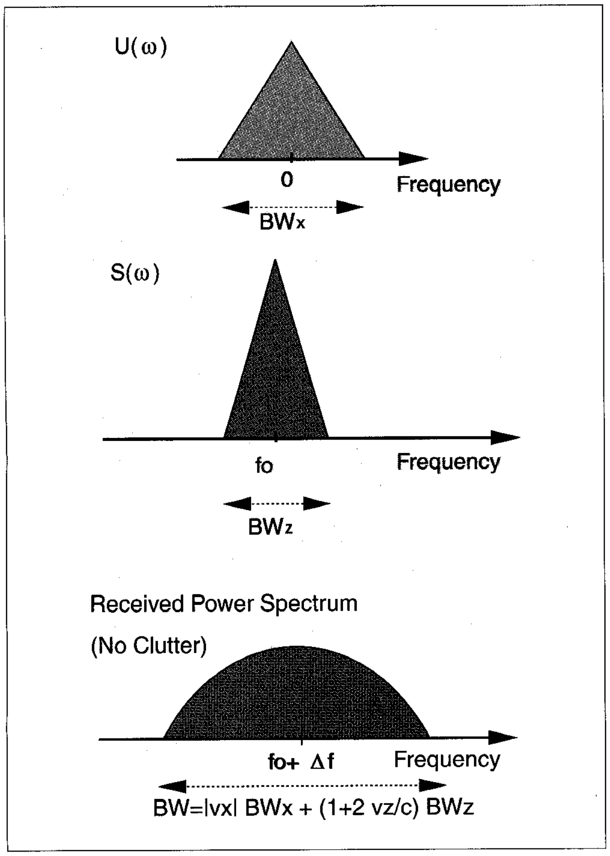

5. Example of the process of velocity estimation from the received power spectrum.

nistic) errors, due to the measurement procedure itself, and *random errors*, due to contamination of the measurables by noise. Random errors can be controlled by taking more measurements and averaging them. On the other hand, deterministic errors are not as easy to eliminate, in general, because they are unique for each problem. These errors can be minimized by optimizing the measurement procedure for the problem at hand, given its associated practical constraints. In the case of flow mapping, the problem is to measure and map true-velocity values in the 2D image plane. Our measurable quantities here are the axial and lateral velocities and their spatial coordinates. We therefore must construct a model for our measurement procedure and consider the optimization of this procedure for the practical imaging time and aperture-size constraints of ultrasound imaging.

Generalized Ambiguity Function Model

Given the similarities that exist between medical ultrasound imaging and radar and sonar imaging, many of the mathematical tools used to study problems in the latter have been adapted to ultrasound imaging. The most important of these tools is the range-Doppler shift-ambiguity function. This function captures the response of a given imaging system as described by the excitation signal. In particular, it defines the resolution in the range direction and the accuracy of the velocity estimation from the Doppler shift (Fig. 6). It is not difficult to see that because of the Fourier uncertainty principle, there will be a trade-off between the improvement in these two directions. As the excitation signal gets longer, the axial resolution becomes worse. On the other hand, a longer signal provides more accurate estimates of the Doppler shift and, hence, the axial velocity. Therefore, it is clear that an ideal ambiguity function of a δ-function form is impossible to achieve. The mathematical description of this problem provides a convenient way of comparing different possible excitation design solutions. Moreover, several successive improvement schemes have been proposed to achieve desirable accuracy levels simultaneously in both the axial resolution and the Doppler shift.

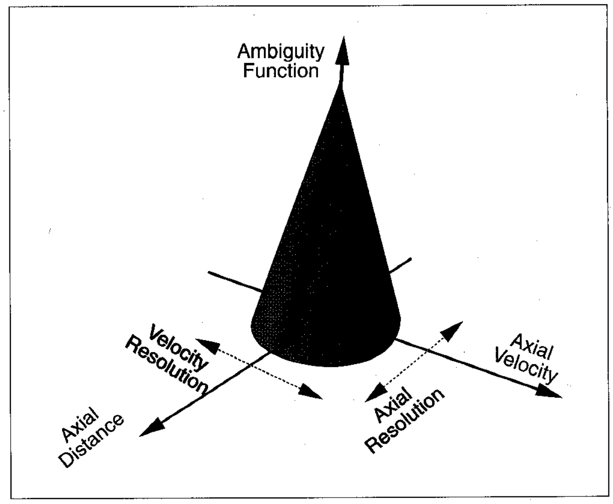

6. Illustration of the ambiguity-function concept.

Although this approach is quite sufficient to describe radar and sonar imaging, it does not provide a complete description of medical ultrasound imaging. The ambiguity function assumes that the Doppler equation model is valid. As we have seen, this model does not generally hold in ultrasound imaging. This means that the lateral resolution and lateral velocity accuracy are left out in the present improvement schemes. Therefore, it is necessary to develop a generalized version of the radar-ambiguity function to devise improvement schemes that take into account the resolution in the 2D image plane, in addition to both components of the true velocity described in our generalized model. In [9], we developed the generalized ambiguity function (GAF) description of the true-velocity flow mapping. We showed that this function is of the form:

$$GAF(x,z,v_x,v_z) = \int_{-\infty}^{\infty} \left[u\left(x^a + v_x^a t\right) \cdot u^*(x + v_x t) \right] \cdot \left[s\left(t\left(1 + \frac{2v_z^a}{c}\right) - \frac{2z^a}{c} \right) \cdot s^*\left(t\left(1 + \frac{2v_z}{c}\right) - \frac{2z}{c} \right) \right] dt$$

where x and z are the location parameters in the transverse and axial directions, respectively; v_x and v_z are the transverse and axial velocities, respectively; (x^a, z^a, v_x^a, v_z^a) are their actual values; $u(\cdot)$ is the effective transmit-receive field function; $s(\cdot)$ is the excitation profile; and c is the ultrasound phase velocity in tissue. As can be seen, the function yields the radar-ambiguity function in the special case when the excitation field is a plane wave. In general, the resolution and velocity accuracy in the axial and lateral directions are coupled. Any successive improvement scheme should be based on combinations of excitation signals

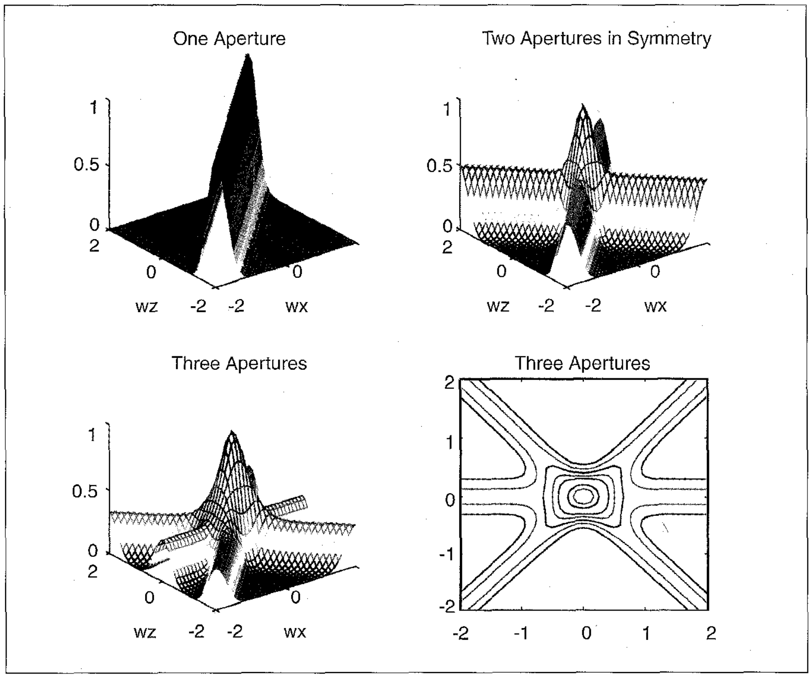

7. Simulation example of a the successive improvement of velocity estimates using more elements from a linear array of circular transducers.

and source apertures. Nevertheless, in some particular choices, the axial or the lateral parts of the GAF may be dominant enough to neglect the effect of the other. In these cases, the conventional schemes based on radar ambiguity can be adapted.

Example of Using GAF

Consider the process of imaging a line of scatterers by using a linear array of transducers and frequency-shift measurements [10]. Assume that the velocity vector is contained in the same plane as the linear array. Notice that the general case can be addressed by a direct generalization of this case when a 2D array is used. Then, the GAF along the axial and lateral velocities takes the form shown in Fig. 7 for different numbers of elements. As can be seen, the geometrical broadening effect becomes smaller as the number of independent transducers increases. The GAF illustration helps to quantify this effect and can be used to choose the number of apertures required to obtain a certain accuracy. It should be noted that in this case, the transit-time broadening can still be described as in the radar-ambiguity function. Therefore, the independent apertures and excitation signals that are required to achieve a particular level of flow-mapping resolution and accuracy can be designed and simulated using the GAF model.

Time-domain Techniques

The second category of flow-mapping techniques performs the estimation process in the time domain from multiple excitations. Let the random pattern of scatterers in the blood be time invariant with regard to the pulse-repetition periods of interest and assume that the blood is moving with a uniform velocity v. Then, the received signal from a single excitation reflects a snapshot of the random pattern at a particular time. Therefore, if we take another snapshot after time T, we will find that this pattern has moved a distance $v \cdot T$. Given that the received signal maps the axial component of this displacement, it is again possible to estimate the axial velocity by detecting the peak of the correlation between the received signals from these two consecutive excitations by using the equation [11-12]:

$$\tau_{peak} = \frac{2 \cdot \Delta r \cdot \cos\theta}{c}$$

Here, τ_{peak} is the time shift of the correlation peak, Δr is the distance traveled by the scattering pattern in the pulse-repetition period T, v_z is the axial velocity, c is the speed of sound in tissue, and θ is the angle of inclination of the flow direction onto the axis of the imaging transducer. As can be seen, this technique is similar to the Doppler equation model in that it provides only one component of the true velocity. Nevertheless, the two techniques differ in two respects: the complexity of computation and the relationship between velocity estimation and mapping resolution. The time-domain technique has a much heavier computational complexity because of the need to compute the correlation function from long RF sample streams. On the other hand, the trade-off between the accuracies of velocity estimation and mapping resolution does not exist in time-domain technique theory — that is, very short excitations can be used to give good resolutions in both dimensions of flow mapping. With the advent of custom-made hardware to handle the large number of computations required in a timely manner by the correlation, time-domain techniques are becoming more appealing as the new standard for flow mapping. However, note that the time-domain methods require at least two successive excitations. Therefore, the total illumination time is double that of the frequency-domain methods, which can theoretically obtain the velocity estimate with one excitation.

The major limitation of time-domain techniques is the difficulty of obtaining true-velocity maps from practical configurations. The theory that supports these techniques assumes that the excitation field is basically a plane wave. To understand the effect of other fields that are used in practice, we develop a generalized model for the flow-mapping process using time-domain techniques.

Generalized Correlation Model

If we start with the same assumptions as in the generalized power-spectrum model, we can show that the correlation function between two consecutive excitations with a pulse-repetition period T is given by [13]:

$$R_{rr}(t, t+\tau) = \lambda^2 \cdot G_1(t) \cdot G_1^*(t+\tau) + \lambda \cdot G_2(t, \tau).$$

Here:

$$G_1(t) = \int_{-\infty}^{\infty} u(r\sin\theta + v_x t) \cdot s\left(t(1 + 2\frac{v_z}{c}) - 2\frac{r\cos\theta}{c} \right) dr$$

and

$$G_2(t) = \int_{-\infty}^{\infty} u(r\sin\theta + v_x t)\cdot u^*((r+\Delta r)\sin\theta + v_x(t+\tau)).$$

$$s\left(t(1+2\frac{v_z}{c}) - 2\frac{r\cos\theta}{c}\right)\cdot s^*\left((t+\tau)(1+2\frac{v_z}{c}) - 2\frac{(r+\Delta r)\cos\theta}{c}\right)dr$$

Notice that $G_2(\cdot)$ is the effective component representing the excitation/field correlation function, while $G_1(\cdot)$ is less important and can be set to vanish by design in many cases [13]. As can be seen, the above expression is rather complex, especially because of the possible coupling between its excitation waveform component and the ultrasound field component. Therefore, we consider important special cases of this expression to illustrate the idea behind the conventional correlation technique. We also suggest a new method of obtaining the true velocity from a single transducer using this technique.

We consider first an ideal plane-wave excitation that has a very brief time duration. Let us approximate this excitation signal by a δ-function. In this case, the correlation function is strongly peaked at a single location as a result of its impulse plus constant form (Fig. 8a). The location of this peak or impulse is given by:

$$\tau_{peak} = \frac{2\cdot\Delta r\cdot\cos\theta}{\left(1+2\frac{v_z}{c}\right)\cdot c} \approx \frac{2\cdot\Delta r\cdot\cos\theta}{c}$$

This expression is the same as the one suggested in the literature. Given the usual difficulty of obtaining a value for θ, this expression has been used to compute the axial velocity as:

$$v_z = \frac{\Delta r\cdot\cos\theta}{T} = \frac{\tau_{peak}\cdot c}{2\cdot T}$$

For most practical cases, the excitation must have a finite time width. This finite time width smears out the single strong peak of the correlation function corresponding to the ideal case (Fig. 8b). This means that the correlation will still have a peak at the same location as in the ideal case, but this peak is not as well defined. Moreover, the strength of this peak gets weaker as the excitation becomes longer. As a result, we would theoretically expect larger peak-detection errors from longer excitations than from brief ones.

Another important special case is when the excitation is a narrow-band signal with a finite time width. This is the usual case in conventional ultrasound imaging. In this case, the correlation function will be narrow-band, with an envelope that has exactly the same form as the smeared-out function in the previous case (Fig. 8c). This brings about the possibility of missing the peak of the correlation function by up to one full excitation period if the peak detection is performed on the correlation function directly. Therefore, we would suggest demodulation of the correlation function to try to eliminate this problem.

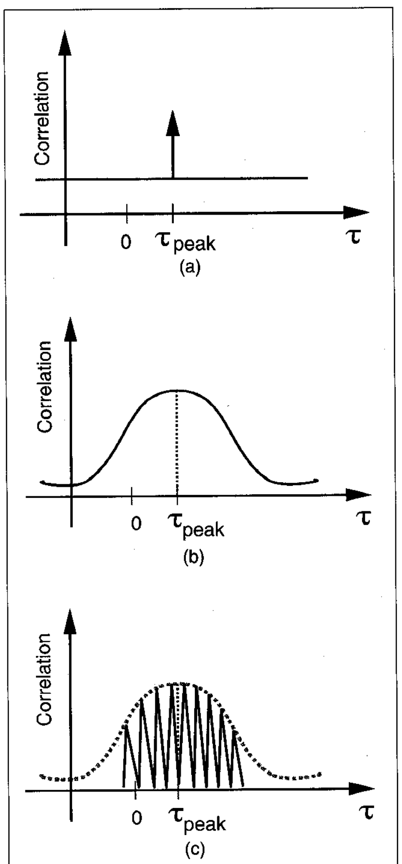

8. Different special cases of the generalized correlation for (a)impulse plane-wave excitation, (b)wide-band plane wave excitation, and (c) narrow-band plane wave excitation.

Let us now consider the general case when both the excitation signal and the field are general functions. In all of the above special cases, the assumption was that the field was a plane wave. The consequence of this assumption is to be able to say that for any pulse repetition period T, the correlation function will have the same form and peak magnitude, but with different shift. This is not true in practice, where strict conditions must be imposed upon T. To understand this, consider the 1D case of a rectangular field. It can be easily seen that after a certain amount of time, all the scatterers that experienced the original excitation will have moved outside this rectangular field. As a result, the correlation between any signals obtained at later times will be completely uncorrelated with the original signal. Therefore, for accurate peak detection, short pulse-repetition periods are desirable to minimize this decorrelation effect.

In spite of the problems associated with this decorrelation effect, we can indeed use it to our benefit by identifying its sources. It can be seen that this effect will depend on both the beam profile at the level of flow, as well as the flow velocity in the lateral direction, which moves the scatterers outside the center of the field. Given the ultrasound field and assuming that we are using circularly symmetric apertures, we can actually derive a formula for the lateral velocity component of the flow in terms of the rate of decorrelation. In particular, we have [13]:

$$v_x = \frac{\alpha}{W_T}$$

Here, W_T is a suitable bandwidth measure for the period between the first excitation and the time when the return signal from an excitation is nearly uncorrelated with the first signal return, while α is a fudge factor that can be determined once the ultrasound field is known and is circularly symmetric. The parameter α also depends on the specific bandwidth measure in use. This method is called *decorrelation tracking,* since it is based on observing several correlation peaks from consecutive excitations (Fig. 9). The lateral velocity is computed from these peaks. Clearly, a minimum of two correlation peaks (three excitations) is required to obtain a lateral-velocity estimate. Nevertheless, more correlation peaks should be used to improve the estimation accuracy. It should be noted that the method of computing the axial velocity remains the same, since in practice, the determination of the peak location is predominantly a function of the axial velocity. Also, as discussed above, it should be kept in mind that the true velocity can be computed from the axial and lateral components based on the symmetry of the field. Hence, using the correlation technique, it is possible to obtain true-velocity maps from a single aperture.

Conclusions

It is possible to reconstruct true-velocity flow maps using ultrasound imaging from a single coplanar aperture by either frequency-domain or time-domain techniques. The advantages of frequency-domain techniques are the relatively lighter load of computations, which allows real-time processing, plus the theoretical possibility of single-shot true-velocity mapping. Nevertheless, these techniques require more excitations from different apertures to achieve good flow-mapping accuracy, as shown by the generalized ambiguity function model. The advantage of the time-domain technique is its relatively higher flow-mapping accuracy with very short excitations. On the other hand, these techniques are computationally extensive and require several excitations to be able to estimate the true velocity. The decision as to which technique to use should take into account their relative advantages/disadvantages in a particular situation.

Acknowledgments

We would like to thank the IDB Merit Scholarship Programme for their financial support. We would like also to thank Dr. Gregory Metzger for his thoughtful comments on the style of this paper. We also appreciate the technical review of this work by Dr. A.M. Youssef of the Systems & Biomedical Engineering Department, Cairo University.

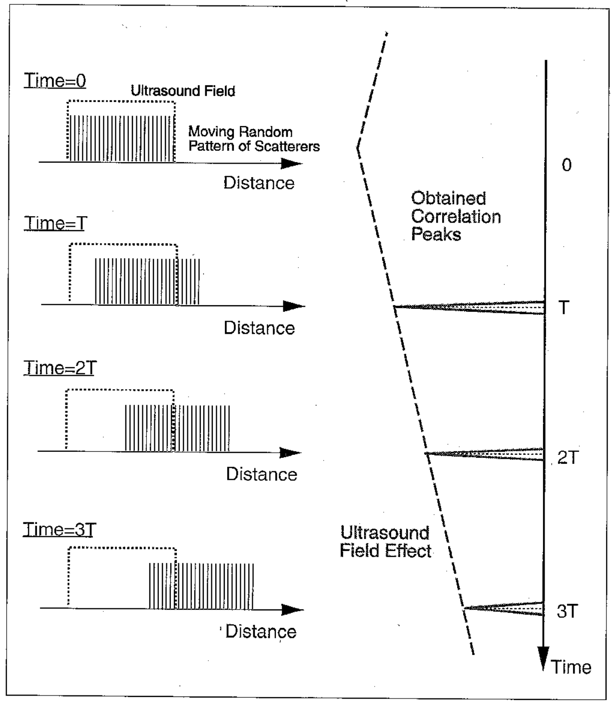

9. Illustration of the concept of the decorrelation tracking technique.

Yasser M. Kadah (Student Member) received his B.Sc. and M.Sc. degrees in biomedical engineering from Cairo University, Egypt, in July 1989 and January 1992, respectively. His main research areas include computed imaging and medical instrumentation. Mr. Kadah is an assistant lecturer with the Systems and Biomedical Engineering department, Cairo University, and is currently on leave of absence to the University of Minnesota to study for a Ph.D. degree with the Biomedical Engineering Program in association with the department of Radiology and the Center of Magnetic Resonance Research (CMRR). Kadah is an active member of the Egyptian Association of Engineers and a founding member of the Egyptian Biomedical Engineers Network (EBENET). He is also a student member of the IEEE EMB, UFFC, and SP societies, and the International Society of Magnetic Resonance in Medicine (ISMRM).

Ahmed H. Tewfik (Fellow IEEE) was born in Cairo, Egypt, on October 21, 1960. He received his B.Sc. degree from Cairo University in 1982 and his M.Sc., E.E. and Sc.D. degrees from the Massachusetts Institute of Technology, Cambridge, MA, in 1984, 1985, and 1987, respectively. Dr. Tewfik has worked at Alphatech, Inc., Burlington, MA, since 1987. He is currently the E.F. Johnson associate professor of Electronic Communications with the department of Electrical Engineering at the University of Minnesota. He served as a consultant to MTS Systems, Inc., Eden Prairie, MN, and is a regular consultant to Rosemount, Inc., Eden Prairie, MN. His current research interests are in the development and application of multiscale techniques and wavelets in the design of high-quality interactive audio, image, and video multimedia databases; optimal data acquisition schemes for radar, magnetic resonance, and ultrasound imaging; stochastic resonance; solutions for local-area communications and high-resolution image synthesis; and industrial measurements.

Dr. Tewfik was elected Fellow of the IEEE in December 1995. He was a principal lecturer at the 1995 IEEE EMBS summer school. He was awarded the E.F. Johnson professorship of Electronic Communications in 1993. He received a Taylor faculty development award from the Taylor foundation in 1992 and an NSF research initiation award in 1990. He gave a plenary lecture at the 1994 IEEE International Conference on Acoustic Speech and Signal Processing (ICASSP'94) and an invited tutorial on wavelets at the 1994 IEEE Workshop on Time-Frequency and Time-Scale Analysis. He was selected to be the first Editor-in-Chief of the *IEEE Signal Processing Letters* in 1993. He is a past associate editor of the *IEEE Transactions on Signal Processing*. and was a guest editor of a special issue of that journal on wavelets and their applications.

Address for Correspondence: Yasser M. Kadah, University of Minnesota, Biomedical Engineering Program, Box 107 UMHC, Minneapolis, MN 55455, phone: (612) 625-5053, fax: (612) 376-9629. E-mail: kadah@sparky.drad.umn.edu.

References

1. **Christensen DA:** *Ultrasonic Bioinstrumentation*, John Wiley & Sons, New York, 1988.

2. **Jones SA:** "Fundamental Sources of Error and Spectral Broadening in Doppler Ultrasound Signals," *Crit. Rev. in Biomed.* Eng., vol. 21, no. 5, pp. 399-483, 1993.

3. **Goodman JW:** *Introduction to Fourier Optics*, McGraw-Hill, 1968.

4. **Shung K and Thieme GA** editors: *Ultrasonic scattering in biological tissues*, CRC Press, Boca Raton, 1993.

5. **Kadah YM and Tewfik AH:** "Space-Invariant True-Velocity Flow Mapping Using Coplanar Observations," *Proc. IEEE EMBC'95*, Montreal, Canada, Sept. 1995.

6. **Cisneros JA, Newhouse VL, and Goldberg B:** "Doppler spectral char-

acterization of flow disturbances in the carotid with the Doppler probe at right angles to the vessel," *Ultras. Med. Biol.*, vol. 11, no. 2, pp. 319-328, 1985.

7. **Censor D. et al:** "Theory of Ultrasound Doppler-Spectra Velocimetry for Arbitrary Beam and Flow Configurations," *IEEE Trans. Biomed. Eng.*, vol. 35, no. 9, pp. 740-751, 1988.

8. **Kadah YM and Tewfik AH:** "Compact Angular Support Beams for Space-Invariant Vector Flow Mapping," *Proc. 1995 Inter. Ultrason. Symp.*, Seattle, Washington, Nov. 1995.

9. **Kadah YM and Tewfik AH:** "Theory of True-velocity Duplex Imaging Using a Single Transducer," *Proc. IEEE ICIP-95*, Washington D.C., Oct. 1995.

10. **Kadah YM and Tewfik AH:** "Waveform and Beamform Design for Doppler Ultrasound Vector Flow Mapping," "True Velocity Estimation Using the Correlation Technique," *Proc. IEEE EMBC'95*, Montreal, Canada, Sept. 1995.

11. **Hein I and O'Brien WD Jr:** "Current Time-Domain Methods for Assessing Tissue Motion by Analysis from Reflected Ultrasound Echoes-A Review," *IEEE Trans. Ultrason. Ferr. Freq. Con.*, vol. 40, no. 2, March 1993.

12. **Foster S, Embree P and O'Brien WD Jr:** "Flow Velocity Profile via Time-Domain Correlation: Error Analysis and Computer Simulation," *IEEE Trans. Ultrason. Ferr. Freq. Con.*, vol. 37, no. 2, May 1990.

13. **Kadah YM and Tewfik AH:** "True Velocity Estimation Using the Correlation Technique," *Proc. 1995 Inter. Ultrason. Symp.*, Seattle, Washington, Nov. 1995.

CLASSIFIED RECRUITMENT

DIRECTOR OF THE CENTER FOR BIOENGINEERING at the University of Washington

The University of Washington seeks a candidate for the position of Director of the Center for Bioengineering. The occupant will hold a tenured professorial rank in the Center for Bioengineering, which is in both the College of Engineering and the School of Medicine. The Director will lead actively to further develop the research and teaching programs of the Center. The Center for Bioengineering has active research programs in biomaterials, biomechanics, cellular bioengineering, biomedical systems, molecular bioengineering, biomedical imaging and biomedical instrumentation. Its graduate program serves more than 100 students of whom the majority are pursuing doctoral degrees. Its undergraduate program serves a small number of superb students who intend to enter either M.D. or M.D./Ph.D. programs. The Center has 30 core faculty, 35 adjunct faculty and 20 affiliate faculty. The Center for Bioengineering has strong collaborative ties with colleagues in the School of Medicine and the College of Engineering.

Nominations and applications should be submitted to Professor Youngmin Kim, Chair of the Bioengineering Director Search Committee, Department of Electrical Engineering, BOX 352500, University of Washington, Seattle, WA 98195-2500. Review of applications will begin on September 1, 1996, and applications will be received until the position is filled. Applications should include a curriculum vita, a statement of interests and goals, and the names of five references.

The University of Washington is building a culturally diverse faculty and strongly encourages applications from female and minority candidates. The University is an Equal Opportunity/Affirmative Action employer.

Assistant Professor in Biomedical Engineering

The Biomedical Engineering Department, of the College of Engineering, University of Miami invites nominations or applications for a tenure seeking position of Assistant Professor in Biomedical Engineering. It is expected that candidates will hold a doctoral degree in biomedical or electrical engineering, with a strong background in biomedical instrumentation with design experience, and have at least 3 yrs academic and/or industrial experience. The applicant is expected to develop & teach upper level undergraduate courses, develop collaborative research with faculty in the College of Engineering and School of Medicine, as well as develop strong ties with the local BME industry. The Department offers BS, MS, Ph.D programs. The University is located in Coral Gables, within the Miami metropolitan area. Nominations and applications with the names of three references should be sent to Dr. Michael Sacks, Dept. of Biomedical Engineering, PO Box 248294, University of Miami, Coral Gables, Florida 33124-0621. The University of Miami is an EQUAL OPPORTUNITY/AFFIRMATIVE ACTION EMPLOYER.

FACULTY POSITION
Bioengineering Program, Texas A&M University

The Bioengineering Program at Texas A&M University has an open position for a tenure track faculty member. Candidates would be expected to develop or maintain an independent funded research program, teach existing courses at both the undergraduate and graduate level, and develop new graduate courses in their speciality area. The desired area of teaching emphasis is in biomechanics. A Ph.D. in biomedical engineering or a closely related field is required. Rank and salary will be commensurate witih background and experience. A starting date of January, 1997 is available, but later starting dates will also be considered.

The Bioengineer Program offers an ABET accredited undergraduate degree and graduate degrees at the masters and doctoral levels. Current areas of research include optical biosensors, optical tomography and spectroscopy, laser interaction with tissue, biomechanics, orthopedic devices, biosignal processing and rehabilitation engineering.

To apply submit a resume and the names of three references to: William A. Hyman, Chair, Search Committee, Bioengineering Program, Texas A&M University, College Station, Texas 77843-3120, 409-845-5532, FAX 409-847-9005, e-mail: search@aggie.tamu.edu.